Fatigue and Overloading Behavior of Steel-Concrete Composite Flexural Members Strengthened with High Modulus CFRP Materials

M. Dawood[1], S. Rizkalla[2] and E. Sumner[3] Civil, Construction and Environmental Engineering, North Carolina State University, Raleigh, NC, 27695-7533

ABSTRACT

Due to corrosion and the continuous demand to increase traffic loads, there is a need for an effective system which can be used to repair and/or strengthen steel bridges and structures. This paper describes an experimental program, recently completed, to investigate the fundamental behavior of steel-concrete composite scaled bridge beams strengthened with new high modulus carbon fiber reinforced polymer (HM CFRP) materials. The behavior of the beams under overloading conditions and fatigue loading conditions was studied as well as the possible presence of shear-lag at the interface of the steel surface and the CFRP strengthening material. The test results are compared to an analytical model based on the fundamental principles of equilibrium and compatibility, to predict the behavior of the strengthened steel-concrete composite beams. Based on the findings of this research work, combined with other work in the literature, a design guideline is proposed for the use of HM CFRP for strengthening the steel flexural members typically used for bridges and structures.

[1] Graduate Research Assistant, Constructed Facilities Laboratory, North Carolina State University, 2414 Campus Shore Dr., Campus Box 7533, Raleigh, NC, 27695-7533

[2] Distinguished Professor of Civil Engineering and Construction, Constructed Facilities Laboratory, North Carolina State University, 2414 Campus Shore Dr., Campus Box 7533, Raleigh, NC, 27695-7533

[3] Assitant Professor, Constructed Facilities Laboratory, North Carolina State University, 2414 Campus Shore Dr., Campus Box 7533, Raleigh, NC, 27695-7533

INTRODUCTION

The use of fiber reinforced polymer (FRP) materials has become a common practice for the repair and strengthening of concrete structures and bridges. Due to the success of this technique, several researchers have also investigated the use of externally bonded CFRP materials for the repair and strengthening of steel bridges and structures. A number of different approaches have been investigated to assess the effectiveness of using CFRP materials for rehabilitation of steel bridge girders including repair of naturally deteriorated girders (Mertz and Gillespie, 1996), repair of overloaded girders (Sen et al., 2001), strengthening of undamaged girders (Tavakkolizadeh and Saadatmanesh, 2003c) and repair of girders with simulated corrosion damage (Al-Saidy et al., 2004). Other research has been conducted to study the fatigue durability of CFRP strengthening systems (Miller et al., 2001).

Early research focused on the use of conventional modulus CFRP materials to repair naturally corroded bridge girders (Mertz and Gillespie, 1996). The research findings indicated that CFRP materials can be effectively used to restore the stiffness and flexural capacity of the damaged girders to levels comparable to those of the undamaged girders.

Researchers have also investigated the use of conventional CFRP materials to repair steel-concrete composite bridge girders which were damaged due to severe overloading conditions (Sen et al., 2001). The CFRP strengthening system helped to increase the nominal capacity of the beams by up to 52 percent. The presence of the CFRP also substantially increased the yield load and post-elastic stiffness of the strengthened beams.

In another study, three undamaged steel-concrete composite beams were strengthened with one, three and five layers of CFRP strips respectively (Tavakkolizadeh and Saadatmanesh, 2003c). The CFRP materials increased the nominal capacity of the strengthened beams by up to 76 percent, however, the increase of the elastic stiffness was

minimal. In a related study, the tension flange of three other steel-concrete composite beams were notched with a 1.3 mm wide notch at midspan to simulate 25, 50 and 100 percent loss of the area of the tension flange (Tavakkolizadeh and Saadatmanesh, 2003b). The repair restored the elastic stiffness and nominal capacity of the girders to levels comparable to the undamaged beams and helped in reducing the residual deflections due to overloading conditions.

Other researchers have simulated corrosion damage by removing a uniform portion of the tension flange along the entire length of the girders (Al-Saidy et al., 2004). CFRP materials were subsequently used to repair the girders. The technique restored the lost strength of the damaged beams to levels higher than those of the undamaged girders. However, only 50 percent of the lost stiffness of the beams was recovered.

Investigations on the fatigue durability of steel beams strengthened with CFRP materials have been limited. Tavakkolizadeh and Saadatmanesh (2003a) demonstrated that installation of externally bonded CFRP patches can reduce crack propagation rates and increase the fatigue life of cracked steel members. Prestressing CFRP patches prior to installation can help promote crack-closure effects and further extend the fatigue life of cracked steel members (Bassetti et al., 2000). The fatigue durability of naturally corroded steel bridge girders, which were repaired with CFRP materials, has been shown to be at least equal to that of many typical steel details which are commonly used in current bridge construction (Miller et al., 2001).

The majority of the previous research has focused on the use of conventional modulus CFRP materials for the repair of steel bridge members. While substantial strength increases have been achieved, typically a large amount of CFRP materials was required to achieve an increase of the elastic stiffness of the beams. This is due to the relatively low modulus of elasticity of the CFRP as compared to steel and also possibly due to the presence of shear-lag

effects between the steel beam and the CFRP materials (Tavakkolizadeh and Saadatmanesh, 2003c).

Recently, high modulus CFRP materials have become commercially available which have a modulus of elasticity approximately twice that of conventional steel. The effectiveness of using HM CFRP materials to repair steel bridge girders was demonstrated by testing three large-scale steel-concrete composite beams strengthened with different configurations of HM CFRP materials (Schnerch, 2005). The elastic stiffness and nominal moment capacity of the beams were increased by up to 36 percent and 45 percent respectively. The testing demonstrated that prestressing the HM CFRP strips prior to installation on the steel beam increased the efficiency of utilization of the CFRP. Test results indicated that prestressing of the HM CFRP required only half the amount of prestressed laminates that was required for a similar beam strengthened with unstressed CFRP laminates to achieve a similar increase of the stiffness. The use of prestressed laminates also helped to maintain the original ductility of the unstrengthened member.

This paper presents the findings of an experimental investigation, recently completed, to study the behavior of steel-concrete composite beams strengthened with HM CFRP materials and subjected to overloading and fatigue loading conditions. The research examined also, the possible presence of shear-lag at the interface between the steel surface and the CFRP materials. The paper also provides an analytical model, based on equilibrium and compatibility principles, to predict the response of steel and steel-concrete composite flexural members strengthened with CFRP materials. A detailed description of the research program presented in this paper is given in Dawood (2005). Based on the research findings and the available literature review, a guideline is proposed which can be used by practitioners to design the required HM CFRP strengthening system for a given steel-concrete composite beam.

HM CFRP STRENGTHENING SYSTEM

The carbon fiber reinforced polymer materials used in this study consist of pitch based carbon fibers pultruded into 4 mm thick, 100 mm wide laminates. The modulus of elasticity and ultimate strain of the strips reported by the manufacturer were 460,000 MPa and 0.00334 respectively. The reported ultimate strain was lower than that measured in the experimental program reported in this paper. The laminates had a fiber volume fraction of 70 percent and were fabricated with a glass fiber peel ply on both faces to minimize the need for surface preparation of the composite material. The strips were bonded to the tension flange of the steel beams using a two part epoxy adhesive with a fast hardener. This adhesive was selected from among six adhesives considered in the same research program (Schnerch, 2005). The tension flange of the steel beam was grit blasted immediately prior to installation of the strengthening system to remove any rust and mill scale from the surface. The surface was subsequently cleaned by air blowing and solvent wiping. After the CFRP strips were installed a wooden clamping system was applied for at least 12 hours until the adhesive had thoroughly set. The adhesive was allowed to cure for at least one week prior to testing.

EXPERIMENTAL PROGRAM

The experimental program consisted of seven steel-concrete composite beams, five of which were strengthened with full-length HM CFRP strips, to study the behavior of the proposed HM CFRP strengthening system under the effect of overloading and fatigue loading conditions. In the first phase three beams were tested to study the behavior of the strengthening system under overloading conditions. The three beams tested in the second phases were used to study the behavior under fatigue loading conditions and to investigate the durability of the strengthening system. The effect of the adhesive thickness on the fatigue behavior was also examined. In the third phase, the seventh beam was tested to examine the

shear-lag phenomenon at the interface of the steel surface and the CFRP materials. The strengthened beams, tested in the first and second phase, were also used to investigate the possible presence of shear-lag phenomenon. The tested beams were designed to represent scaled steel-concrete composite beams which are typically used for highway bridge construction. The cross-section of the tested beams is shown schematically in Fig 1. The beams were strengthened with different reinforcement ratios, ρ, of HM CFRP materials and tested in a four point bending configuration as shown schematically in Fig 2(a) and Fig 2 (b).

A detailed description of the three phases of the experimental program is presented in Table 1. A total of three beams were tested to investigate the behavior under overloading conditions. Two of the test beams were strengthened with two different levels of CFRP to investigate the effect of the CFRP reinforcement ratio on the behavior of the beams. A third unstrengthened beam was tested to serve as a control beam for the overloading study. All three of the beams were unloaded and reloaded at various load levels to simulate the effect of severe overloading conditions.

The objective of the fatigue study was to verify the fatigue durability of the strengthened beams and to assess the effect of the bond preparation on the fatigue durability of the strengthening system. Three additional beams were tested. Two of the beams were strengthened with the same amount of CFRP materials, however, using different bonding techniques. The first beam was strengthened using the standard bonding procedure described previously. The second beam was strengthened using a modified bonding technique which included increasing the thickness of the adhesive layer which was applied in conjunction with a primer coat of a silane adhesion promoter. The third beam remained unstrengthened and was used as a control beam for the fatigue study. All three beams were subjected to three million fatigue loading cycles and the load was cycled at a frequency of 3 Hz. The minimum applied load used for the cycled loading, P_{min}, was selected to be equivalent to 30 percent of

the calculated yield load of the unstrengthened beams to simulate the effect of the sustained dead-load for a typical bridge structure. The maximum load applied, P_{max}, for the unstrengthened beam, was selected to be equivalent to 60 percent of the calculated yield load to simulate the combined effect of dead-load and live-load. The maximum load for the two strengthened beams, P_{max}, however, was selected to be equivalent to 60 percent of the calculated increased yield load of the strengthened beams. The resulting load range, ΔP, also simulated an increase of 20 percent of the allowable live-load level in comparison to the unstrengthened beam.

To simulate the actual behavior of a typical strengthened highway bridge, the two strengthened beams that were tested in the fatigue study were subjected to a sustained simulated dead-load prior to installation of the HM CFRP strengthening system. The simulated dead-load was applied using an independent loading system as shown in Fig 3. Prior to installation of the CFRP, the simulated dead-load of 50 kN was applied by tightening the nuts against the load cells on the threaded rods. The simulated dead-load was sustained on the beams while the CFRP strips were installed and during the curing process of the adhesive. After the adhesive cured, the load was transferred from the independent dead-load system to the hydraulic actuator and the fatigue loading program was commenced.

The seventh beam, tested in the third phase, was tested under monotonic loading conditions up to failure to investigate the shear-lag phenomenon independent of the effect of overloading or fatigue loading conditions. The strain measurements of the four strengthened beams, tested in the first and second phases, were also used to examine the shear-lag phenomenon.

The tensile yield strength and modulus of elasticity of the steel beams were determined by standard coupon tests and were found to be 380 MPa and 200,000 MPa respectively. The compressive strength of the concrete, used for the concrete deck slabs for

the seven test beams, was determined from standard cylinder tests after 28 days. The measured concrete cylinder strengths for the deck slabs used for the different test beams are given in Table 1.

All of the test beams were instrumented to measure deflections at midspan and at the support locations. All of the test beams were also instrumented to measure strain at several depths along the midspan cross-section. The two strengthened beams which were tested in the fatigue study, were also instrumented to measure strain at the quarter-span cross-section. The measured strains were used to construct the strain profiles for the strengthened beams to investigate the shear-lag phenomenon at the interface between the steel surface and the CFRP materials.

EXPERIMENTAL RESULTS

This section presents and discusses the test results of each of the three phases considered in the experimental program and summarizes the relevant research findings.

Overloading Study

The load-deflection relationships of the three beams that were tested to study the overloading behavior of the strengthened beams are presented in Fig 4. The behavior of the control beam, beam ST-CONT, is given in Fig 4(a) while the behavior of the other two beams, strengthened with 4.3 and 8.6 percent reinforcement ratios of HM CFRP, are given in Fig 4(b) and Fig 4(c) respectively. All three beams were unloaded and reloaded at various loading stages to simulate the effect of overloading conditions.

In general, the load-deflection behavior of the three beams was essentially linear up to yielding of the steel. Prior to yielding of the steel all three of the tested beams exhibited minimal residual deflections upon removal of the applied load.. Reloading resulted in minimal hysteresis in all cases. After yielding of the steel, the unstrengthened beam exhibited

a significant increase of the measured residual deflection, as shown in Fig 4(a), while the two strengthened beams continued to exhibit minimal residual deflections up to rupture of the CFRP. A typical rupture failure of the HM CFRP laminates is shown in Fig 4(d). After rupture of the CFRP occurred, the load-deflection response of the strengthened beams followed a similar trend to that measured for the unstrengthened beam. The tests indicate that the nominal capacity of the unstrengthened beam, ST-CONT, was governed by crushing of the concrete while the nominal capacity for the two strengthened beams, OVL-1 and OVL-2 was governed by rupture of the CFRP.

The increases of the elastic stiffness, yield load and nominal strength of the two strengthened beams are presented in Table 2. The elastic stiffness, yield load and nominal capacity of the beams were increased by 46 percent, 85 percent and 66 percent respectively using the higher reinforcement ratio. Inspection of Table 2 indicates that doubling the CFRP reinforcement ratio, from 4.3 percent to 8.6 percent, approximately doubled the elastic stiffness increase of the beams. Doubling the reinforcing ratio also approximately tripled the increase of the measured yield load and nominal capacity of the strengthened beams. This demonstrates that increasing the reinforcement ratio increases the efficiency of the CFRP material.

In addition to the increase of the stiffness and strength, use of the HM CFRP materials also helped to reduce the residual deflection of the strengthened beams due to possible overloading conditions of the beams. To evaluate the effectiveness of the HM CFRP strengthening system, each of the three beams was unloaded at a load level of 175 kN to study the behavior under possible overloading conditions. This load is equivalent to the allowable service load for the beam strengthened with the higher HM CFRP reinforcement ratio of 8.6 percent and induced a strain level of 60 percent of the yield strain of the steel, ε_y, as determined from the coupon tests. The average measured strain at the steel tension flange at

this load level was 2.5 ε_y, 1.0 ε_y and 0.6 ε_y for beams ST-CONT, OVL-1 and OVL-2 respectively. The beams were unloaded to a load level of 45 kN which simulates an equivalent sustained load acting on a typical bridge after an overloading event due to the effect of self-weight and superimposed dead-load. The plastic residual deflection, at the 45 kN load level for beams OVL-1 and OVL-2 were respectively 20 percent and 15 percent of the measured residual deflection of beam ST-CONT. Consequently, under severe overloading conditions, an unstrengthened beam may require replacement while a strengthened beam may remain in excellent service condition.

Fatigue Study

Three beams were tested in the fatigue study. Beams FAT-1 and FAT-1b were strengthened with 4.3 percent reinforcement ratio of CFRP using two different bonding techniques while beam FAT-CONT remained unstrengthened to serve as a control beam for the fatigue study. The two strengthened beams were tested under an equivalent load to simulate a 20 percent increase of the applied live load as compared to the unstrengthened beam. All three beams sustained a three million-cycle fatigue loading course without exhibiting any indication of failure. The degradation of the stiffness and mean deflection of the three beams throughout the three million-cycle loading course are shown in Fig 5(a) and (b) respectively. The stiffnesses and mean deflections presented in the figure are normalized with respect to the measured initial values at the beginning of the fatigue loading program.

All three of the tested beams exhibited a minimal degradation of the elastic stiffness of less than 5 percent throughout the three million fatigue loading cycles as shown in Fig 5(a). However, the unstrengthened beam FAT-CONT exhibited nearly a 30 percent increase of the mean deflection due to the applied fatigue cycles. This behavior was most likely due to the fatigue-creep behavior of the concrete deck slab. Both of the strengthened beams exhibited

superior performance with a maximum increase of the measured mean deflection of 10 percent. The observed degradation of the two strengthened beams throughout the three million fatigue cycles was similar. This indicates that neither the bonding procedure nor the adhesive thickness affected the fatigue behavior of the strengthening system.

After the completion of the fatigue program, the three beams were loaded monotonically to failure. The load-deflection behavior of the beams followed a similar trend to the observed load-deflection envelope of the three beams that were tested in the overloading study. The nominal capacity of the two strengthened beams, FAT-1 and FAT-1b, was governed by rupture of the CFRP at a load of 250 kN. After rupture of the CFRP, the load-deflection behavior of the two beams followed a similar trend to the load-deflection behavior of the unstrengthened beam, FAT-CONT. Crushing of the concrete for all three beams occurred at a measured load of between 200 kN and 215 kN. The findings of the fatigue study demonstrate that the strengthened beams can sustain the specified increase of the live load level for the selected HM CFRP reinforcement ratio while maintaining a level of durability which was comparable to that of the unstrengthened beam.

Shear-lag Study

One additional beam, SHL, was tested to investigate the possible presence of a shear-lag phenomenon at the interface of the steel surface and the CFRP materials under monotonic loading conditions. The beam was strengthened with 8.6 percent reinforcement-ratio of HM CFRP. The load-deflection behavior of beam SHL was essentially the same as the load-deflection envelope of beam OVL-2, shown in Fig 4(c), which was strengthened with the same reinforcement ratio of HM CFRP.

The measured strain profiles at midspan of beams SHL and OVL-2, immediately prior to rupture of the HM CFRP material, are shown in Fig 6. The measured strain profiles for

both beams indicate a slight discontinuity of the strain profile at the interface of the bottom surface of the steel tension flange and the CFRP material. However, the opposite sign of the discontinuity suggests that the discontinuity is not due to the presence of a shear lag effect. The measured discontinuity is likely due to the effect of residual stresses in the steel beam during the manufacturing process or due to possible local instability and lateral movement of the tension flange of the steel beam during the test. The presence of these effects was confirmed by independent strain measurements at different locations along the steel tension flange of the strengthened and unstrengthened test beams. The measured strain profiles for the remaining three strengthened test beams, OVL-1, FAT-1 and FAT-1b, were essentially linear and exhibited minimal discontinuities between the steel and the CFRP. The findings of the shear-lag study indicate that the effect of shear-lag is negligible and the plane sections remain plane assumption is appropriate for the analysis of the strengthened beams.

ANALYTICAL MODEL

The analytical model proposed to predict the load-deflection behavior of the strengthened steel-concrete composite beams is based on equilibrium and compatibility. The model considers the non-linear material characteristics of the steel and the concrete and assumes linear-elastic behavior for the CFRP materials. The procedure is described briefly below and is presented in detail elsewhere (Dawood, 2005; Schnerch, 2005; Schnerch et al., 2006).

The moment-curvature behavior for a given cross-section is determined based on a selected strain at the top level of the compression flange and iteration of the neutral axis depth. For a given strain at the top surface of the concrete deck, and an assumed neutral axis depth, the strain at any level in the cross-section can be calculated using an assumed linear strain profile. The known material characteristics can be used to calculate the stress distribution throughout the cross section. The internal forces are calculated by integration of the stress

profile. The neutral axis depth can then be determined through iteration until horizontal force equilibrium is satisfied and the corresponding moment and curvature of the section can be calculated for the given strain level. The strain at the top of the section is incremented to establish the complete moment-curvature relationship of the section. For a given loading and support configuration the load deflection behavior of the beam can be determined by integration of the curvature profile using any commonly accepted method.

The nominal capacity of the strengthened section is limited by rupture of the CFRP which occurs when the strain at the level of the CFRP approaches the maximum value. After rupture of the CFRP the behavior of the beam can be described by considering the unstrengthened section up to crushing of the concrete deck slab. The model assumes that the capacity of the adhesive joint is adequate to develop the full tensile capacity of the CFRP materials and, consequently, debonding is not considered as a possible mode of failure. An independent analytical model which can be used to determine the shear and normal bond stresses in the adhesive joint of a strengthened beam is presented in a separate paper by Schnerch (2005).

Validation of the Analytical Model

The accuracy of the analytical model was verified by comparing the predicted load-deflection response to the measured values obtained from the experimental program. The material properties to be input into the analytical model were determined by testing of representative material samples. The load-deflection response of the strengthened test beams was predicted and compared to the measured values obtained from the experimental program.

The material properties of the concrete deck slabs for the five beams were determined by testing representative concrete cylinders. The complete stress-strain relationship of the cylinders was measured and a best fit curve to the measured data was established using the

equation presented in Fig 7 (Collins and Mitchell, 1997) where f_c is the stress in the concrete corresponding to a strain, ε; ε_c' is the strain corresponding to the peak concrete stress, f_c'; n is a curve fitting factor and k is a post peak decay factor. The measured stress-strain relationships for the cylinder tests, as well as the best fit curves for all three batches of concrete are presented in Fig 7. The material characteristics used for the concrete material model are presented in Table 3. The longitudinal steel reinforcement in the concrete slab was modeled using an elastic-plastic relationship with an elastic modulus of 200,000 MPa and a yield strength of 400 MPa.

The modulus of elasticity and yield strength of the structural steel W-sections were determined from representative coupon tests as 200,000 MPa and 380 MPa as discussed previously. However, all of the beams that were tested in the experimental program exhibited an earlier deviation from the elastic behavior due to the presence of residual stresses which was not observed in the coupon tests. A tri-linear material model was used to account for the gradual yielding of the steel in the beam tests due to the presence of residual stresses as shown in Fig 8 (Englekirk, 1994). The proportional limit strain, ε_p, for the steel was determined from the measured strain at the tension flange of the steel beams that were tested in the experimental program. The measured load-strain relationship at the tension flange of the beams became non-linear at a measured strain of approximately 0.0016. Consequently, this value was selected as the proportional limit strain for the material model.

The HM CFRP laminates were modeled as a linear-elastic material to failure using the elastic modulus of 460,000 MPa reported by the manufacturer and the average measured strain at rupture of the CFRP strips of 0.0037 from the beam tests.

The predicted and measured load deflection responses based on the proposed model and the measured values for beams OVl-1, OVL-2, FAT-1 and FAT-1b are compared in Fig 9.

Inspection of Fig 9 indicates that the analytical model closely predicts the load-deflection behavior of the strengthened beams prior to rupture of the CFRP. The predicted response of the unstrengthened beams closely matches the measured behavior after rupture of the HM CFRP laminates. The measured and predicted nominal capacity and elastic stiffness increase for each of the five beams are given in Table 4. In all cases the analytical model accurately predicted the nominal capacity and elastic stiffness increase of the strengthened beams to within 10 percent of the measured values.

The analytical model was also used to predict the nominal moment capacity of the tested beams for a number of different reinforcement ratios of CFRP up to 40 percent to establish practical limits for the amount of strengthening which can be applied to a given cross-section. The relationship between the reinforcement ratio and the nominal moment capacity of the strengthened beams is presented in Fig 10 for the specific cross-section considered in the current test program. The test results of the five strengthened beams that were tested in the experimental program are also plotted for reference purposes. From the figure, it can be seen that the relationship is essentially tri-linear and the figure can be separated into three distinct regions. The first region includes reinforcement ratios up to 1.5 percent which corresponds to installing a 100mm wide x 0.5 mm thick CFRP strip on the tension flange of the steel beam. This represents a very under-reinforced section for which rupture of the CFRP occurs prior to achieving the nominal strength of the unstrengthened section, $M_{n,US}$. Within this region installation of the CFRP does not increase the nominal capacity of the section. As such, this represents a practical lower limit of effectiveness for the allowable amount CFRP strengthening which should be applied to the beam.

For reinforcement ratios from 1.5 percent to 20 percent the nominal capacity of the section is governed by rupture of the CFRP prior to crushing of the concrete. Increasing the reinforcement ratio within this region results in a corresponding increase of the nominal

capacity of the strengthened section, $M_{n,S}$ up to 2.6 times the nominal capacity of the unstrengthened member. All of the tested beams fall within this region as indicated in Fig 10. The failure of the section by rupture of the CFRP in this region indicates full utilization of the capacity of the CFRP materials.

The third region includes sections with a reinforcement ratio of CFRP greater than 20 percent. This corresponds to installing a 100mm wide x 7 mm thick CFRP strip on the tension flange of the beam. In this region failure of the section occurs due to crushing of the concrete prior to rupture of the CFRP. The slight increase of the strength in this region is mainly due to the shift of the neutral axis by increasing the amount of CFRP applied to the beam. This represents a practical upper limit for the reinforcement of the cross-section in this study. From the figure it can be seen that increasing the reinforcement ratio beyond this limit does not significantly increase the nominal capacity of the section indicating inefficient utilization of the CFRP strengthening materials.

While the relationship shown in Fig 10 and the limits discussed above are for the specific beam cross-section considered in this study, a similar behavior can be expected for most typical bridge girders which consist of a relatively slender steel-section and a typical reinforced concrete deck. Similar limits can be easily established for any steel-concrete composite beam configuration using the presented analytical model.

DESIGN GUIDELINES

Based on the findings of this research program a series of design guidelines have been developed and proposed for the design of HM CFRP strengthening for steel-concrete composite beams. A detailed description of the proposed flexural design procedures is given by Schnerch et al. (2006).

The design procedure requires that the increase of live load for a steel-concrete composite beam strengthened with HM CFRP materials should satisfy three criteria. These three criteria are shown in Fig 11 with respect to the moment-curvature response of a typical strengthened beam. Due to the presence of the additional layer of HM CFRP material, the yield moment of the strengthened beam, $M_{Y,S}$, is greater than the yield moment of the same beam prior to strengthening, $M_{Y,U}$. This was verified by the findings of several experimental studies (Dawood, 2005; Schnerch, 2005). It should be noted that the increase of the yield moment due to installation of the HM CFRP strengthening system is highly dependent on the level of the dead load acting on the member prior to installation of the strengthening. To ensure that the strengthened beam remains elastic under service loading conditions, the total applied moment acting on the strengthened section, including the effect of dead load, M_D, and the increased live-load, M_L, should not exceed 60 percent of the increased yield moment of the strengthened section. To satisfy the strength limit state, the total factored moment based on the appropriate dead-load and live-load factors, α_D and α_L respectively, should not exceed the ultimate moment capacity of the strengthened section, $M_{U,S}$. Also, to ensure that the structure remains safe in the case of possible loss of the strengthening system, the total applied moment, including the effect of dead-load and the increased live-load should not exceed the residual nominal moment capacity of the unstrengthened section, $M_{n,US}$. The fatigue life of the strengthened member under the effect of the increased live load level should be checked to be within the allowable stress range specified by the applicable design codes. The findings of the fatigue study demonstrate that the fatigue durability of the strengthening system under an increased live load inducing a stress range at the tension flange of the steel beam of 30 percent of the yield strength of the steel, was comparable to that of an unstrengthened beam which was tested using the same stress range

While the nominal behavior of the member can be used to predict the behavior under service loading conditions, the design ultimate capacity should incorporate suitable reduction factors to ensure that the member remains safe. Due to the statistical uncertainty of the measured ultimate capacity of the HM CFRP materials, the mean strength of the CFRP reported by the manufacturer, $\bar{f}_{FRP,u}$, should be reduced by 3 times the standard deviation, σ, when calculating the ultimate capacity of the strengthened section (ACI 440.2R, 2002). To account for possible environmental degradation of the CFRP materials, an environmental degradation factor, C_E should also be implemented (ACI 440.2R, 2002). Therefore, the design strength of the HM CFRP material can be calculated as

$$f_{FRP,u} = C_E(\bar{f}_{FRP,u} - 3\sigma) \qquad \text{Equation (1)}$$

Based on the current guidelines of the American Concrete Institute it is proposed that an environmental degradation factor of 0.85 be considered for CFRP materials under outdoor exposure conditions (ACI 440.2R, 2002).

The design failure strain of the CFRP material, $\varepsilon_{FRP,u}$ can be calculated using the calculated design strength of the CFRP and the average elastic modulus, E_{FRP}, reported by the manufacturer.

The nominal capacity of a steel-concrete composite beam strengthened with high modulus CFRP materials is typically governed by rupture of the CFRP materials which occurs in a sudden, brittle manner without significant warning. To account for the brittle nature of failure, a strength reduction factor, ϕ, of 0.75 is recommended. This reduction factor is consistent with the reduction used in the American Institute of Steel Construction (AISC)

LRFD Specification (2001) for rupture type limit states. The design ultimate capacity of the strengthened beam, $M_{U,S}$ should thus be calculated as $\phi M_{n,S}$.

CONCLUSIONS

This paper presents details of an experimental program which was undertaken to investigate the fundamental behavior of steel-concrete composite beams strengthened using high modulus CFRP materials. The findings of the experimental program provide comprehensive evidence that HM CFRP materials can be used to increase the elastic stiffness, yield load and nominal capacity of steel flexural members which are typically used for most highway bridge structures. The presence of the CFRP helps to reduce the residual deflection due to overloading conditions which can help reduce or eliminate the need for repair or replacement of a structure. The tested strengthened beams where able to sustain three million loading cycles with a 20 percent increase of the simulated live load level. The beams exhibited similar performance to a control beam which was tested at a lower loading range. Further, using thicker adhesive and a silane adhesion promoter did not appear to affect the fatigue behavior of the strengthening system. Based on the measured strain profiles of the five strengthened beams which were investigated in the shear-lag study, the effect of shear-lag between the steel beam and the CFRP materials is minimal.

An analytical model is also presented which is based on a moment-curvature analysis and satisfies the conditions of equilibrium and compatibility. The model accurately predicted the load-deflection response, the nominal capacity and the elastic stiffness increase of the tested beams.

Based on the findings of the research program a series of design guidelines are presented which can be used to design the required HM CFRP strengthening for a steel-concrete composite beam. The allowable live load increase for a strengthened beam should satisfy three conditions. Particularly,

(i) $M_D + M_L \leq 0.6\, M_{Y,S}$

(ii) $\alpha_D M_D + \alpha_L M_L \leq M_{U,S}$

(iii) $M_D + M_L \leq M_{n,U}$

The findings of this research demonstrate that externally bonded HM CFRP materials represent an effective strengthening system for steel-concrete composite highway bridge girders.

Acknowledgements

The authors would like to acknowledge the support provided by the National Science Foundation (NSF) Industry/University Cooperative Research Center (I/UCRC) for the Repair of Buildings and Bridges with Composites (RB^2C) and the support provided by Mitsubishi Chemical FP America Inc.

NOTATION

The following symbols are used in this paper:

C_E = environmental reduction factor

f_c = concrete stress

f_c' = peak concrete strength

$f_{FRP,u}$ = design strength of FRP material

$\bar{f}_{FRP,u}$ = mean nominal strength of FRP as reported by manufacturer

k	=	post peak decay factor
M_D	=	moment due to applied dead load
M_L	=	moment due to applied live load
$M_{n,S}$	=	nominal moment capacity of a strengthened section
$M_{n,U}$	=	nominal moment capacity of an unstrengthened section
$M_{Y,S}$	=	yield moment of a strengthened section
$M_{y,U}$	=	yield moment of an unstrengthened section
$M_{U,S}$	=	factored ultimate moment of a strengthened section
$M_{U,U}$	=	factored ultimate moment of an unstrengthened section
n	=	curve fitting factor
P_{max}	=	maximum load in a fatigue cycle
P_{min}	=	minimum load in a fatigue cycle
ΔP	=	fatigue load range
t_a	=	adhesive thickness
α_D	=	dead load factor
α_L	=	live load factor
ε	=	strain
ε_c'	=	concrete strain corresponding to peak concrete stress
ε_{cu}	=	ultimate concrete strain
$\varepsilon_{FRP,u}$	=	design failure strain of FRP material
ε_p	=	steel proportional limit strain
ε_y	=	steel yield strain
ϕ	=	strength reduction factor
ρ	=	reinforcement ratio of FRP

σ = standard deviation

References

Al-Saidy, A.H., Klaiber, F.W. & Wipf, T.J. (2004). "Repair of steel composite beams with carbon fiber-reinforced polymer plates." *Journal of Composites for Construction, 8 (2),* 163-172.

American Association of State Highway and Transportation Officials. (2002). *AASHTO LRFD bridge design specifications,* AAHSTO, Washington, D.C.

American Concrete Institute. (2002). *ACI 440.2R-02 Guide for the design and construction of externally bonded FRP systems for strengthening concrete structures,* ACI, Farmington Hills, MI.

American Institute of Steel Construction. (2001) *Manual of steel construction: load and resistance factor design. Third edition,* AISC, Chicago, IL.

Bassetti, A. Nussbaumer, A. & Hirt, M.A. (2000). Crack repair and fatigue life extension of riveted bridge members using composite materials. In Hosny, A.H. & Bakhoum, M.M. (Eds.), *Bridge engineering conference 2000 past achievements current practices future technologies* (pp. 227-237), Egyptian Society of Engineers, Egypt.

Collins, M. P. and Mitchell, D. (1997) *Prestressed Concrete Structures*. Response Publications, Canada.

Dawood, M. (2005). *Fundamental Behavior of Steel-Concrete Composite Beams Strengthened with High Modulus Carbon Fiber Reinforced Polymer (CFRP) Materials*. Master's Thesis, North Carolina State University, Raleigh, North Carolina.

Englekirk, R. (1994). *Steel structures: Controlling behavior through design*, Wiley, New York.

Mertz, D.R. & Gillespie Jr., J. W. (1996). Rehabilitation of steel bridge girders through the application of advanced composite materials (Contract NCHRP-93-ID011), TRB, Washington, D.C.

Miller, T.C., Chajes, M.J., Mertz, D.R. & Hastings, J.N. (2001). Strengthening of a steel bridge girder using CFRP plates. *Journal of Bridge Engineering, 6 (6),* 514-522.

Schnerch, D. (2005). *Strengthening of steel structures with high modulus carbon fiber reinforced polymer (CFRP) Materials.* Ph.D. dissertation, North Carolina State University, Raleigh, North Carolina.

Schnerch, D., Dawood, M. and Rizkalla, S. (2006). *Design guidelines for the use of HM strips: strengthening of steel-concrete composite bridges with high modulus carbon fiber reinforced polymer (CFRP) strips.* Available from http://www.ce.ncsu.edu/centers/rb2c/Events/RB2CJune05Mtg.htm.

Sen, R., Libby, L. & Mullins, G. (2001). Strengthening steel bridge sections using CFRP laminates. *Composites Part B: Engineering, 39,* 309-322.

Tavakkolizadeh, M. & Saadatmanesh, H. (2003a). Fatigue strength of steel girders reinforced with carbon fiber reinforced polymer patch. *Journal of Structural Engineering, 129 (2),* 186-196.

Tavakkolizadeh, M. & Saadatmanesh, H. (2003b). Repair of damaged steel-concrete composite girders using carbon fiber-reinforced polymer sheets. *Journal of Composites for Construction, 7 (4),* 311-322.

Tavakkolizadeh, M. & Saadatmanesh, H. (2003c). Strengthening of steel-concrete composite girders using carbon fiber reinforced polymer sheets. *Journal of Structural Engineering, 129 (1),* 30-40.

List of Tables

Table 1: Test matrix for the three phases of the experimental program

Beam ID	Reinforcement Ratio[a], ρ	Adhesive Thickness, t_a	Concrete Strength, f_c'	Loading
Overloading				
ST-CONT	0 percent	N/A	44 MPa	unload/reload
OVL-1	4.3 percent	0.1 mm	44 MPa	unload/reload
OVL-2	8.6 percent	0.1 mm	44 MPa	unload/reload
Fatigue				
FAT-CONT	0 percent	N/A	34 MPa	fatigue: P_{min}=50 kN, ΔP=50 kN
FAT-1	4.3 percent	0.1 mm	34 MPa	fatigue: P_{min}=50 kN, ΔP=60 kN
FAT-1b[b]	4.3 percent	1.0 mm	58 MPa	fatigue: P_{min}=50 kN, ΔP=60 kN
Shear-lag				
SHL	8.6 percent	0.1 mm	44 MPa	monotonic

[a]defined as the ratio of the cross-sectional area of the CFRP strengthening, accounting for the fiber volume fraction to the cross-sectional area of the steel beam

[b]included the use of a silane adhesion promoter

Table 2: Comparison of the overloading beams

Beam ID	Reinforcement Ratio, ρ	Stiffness Increase	Yield Load Increase	Capacity Increase
ST-CONT	0 %	N/A	N/A	N/A
OVL-1	4.3 %	27 %	32 %	20 %
OVL-2	8.6 %	46 %	85 %	66 %

Table 3: Coefficients for the concrete material model

Coefficient	Batch 1	Batch 2	Batch 3
Peak strength, f_c'	44 MPa	34 MPa	58 MPa
Strain at peak, ε_c'	0.0035	0.0035	0.0038
Fitting factor, n	4.77	2.84	4.25
Post peak factor, k	1.13	1.22	1.92
Ultimate strain, ε_{cu}	0.0045	0.0049	0.0043

Table 4: Comparison of measured and predicted nominal capacities and elastic stiffness

Beam	Nominal Capacity		Stiffness Increase	
	Measured	Predicted	Measured	Predicted
OVL-1	259 kN	270 kN	27%	27%
OVL-2	357 kN	366 kN	46%	48%
SHL	358 kN	366 kN	[a]	48%
FAT-1	250 kN	264 kN	40%	32%
FAT-1b	252 kN	272 kN	35%	26%

[a] Unstrengthened stiffness of beam SHL was not measured

Table of Figures

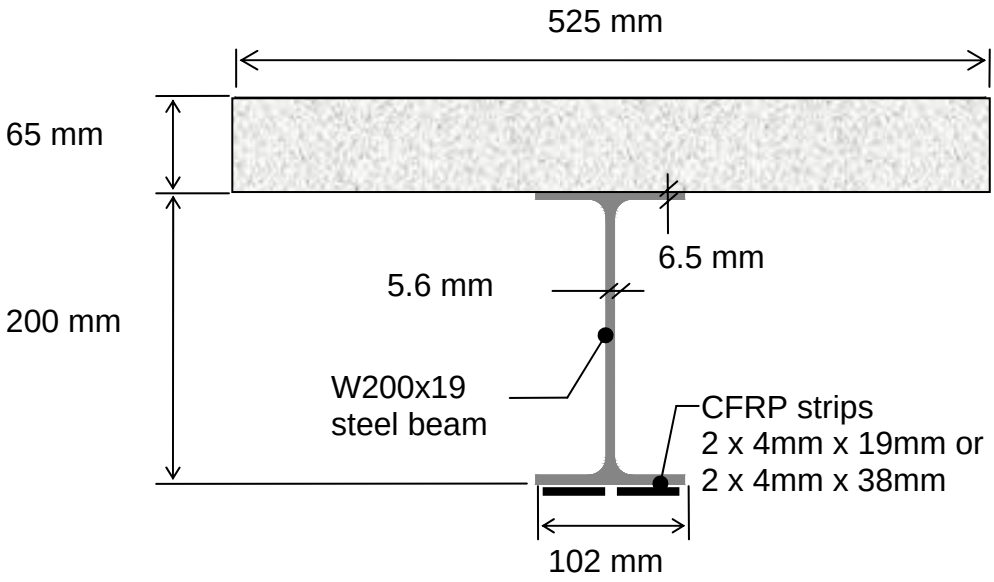

Fig 1: Cross-section of a typical test beam

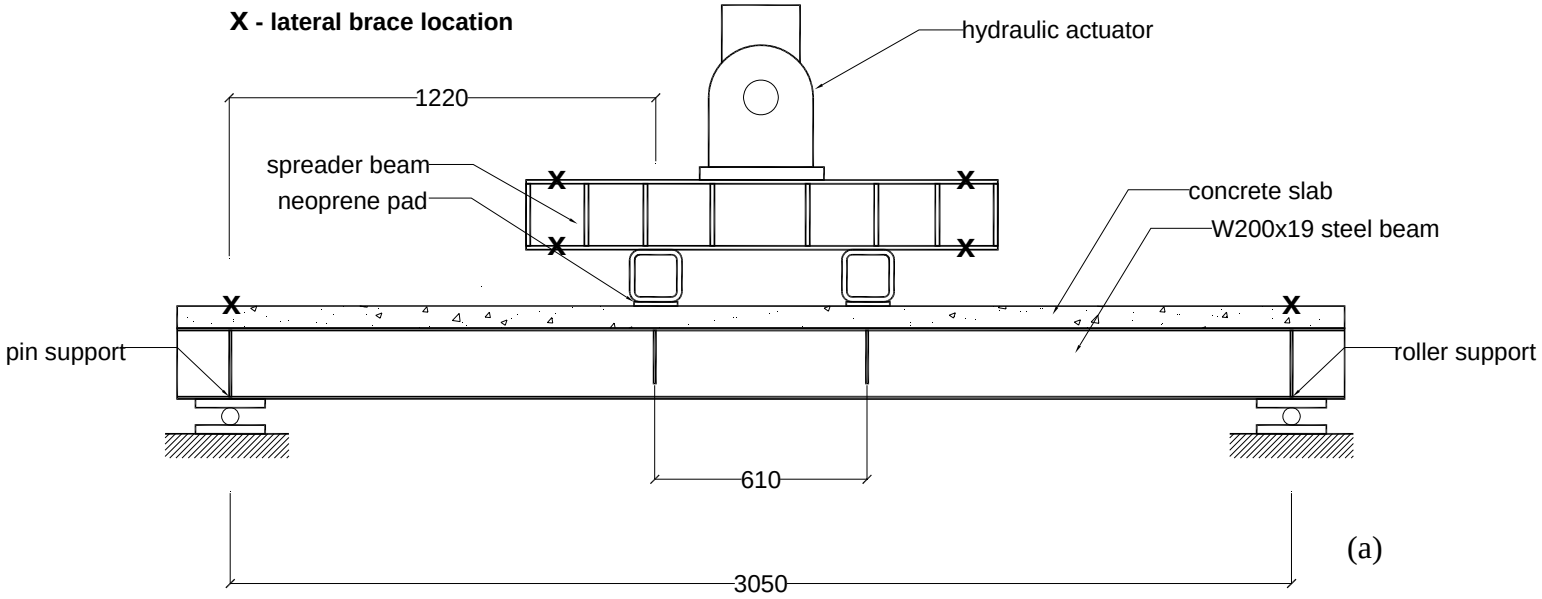

Fig 2: Beam test setup (a) schematic

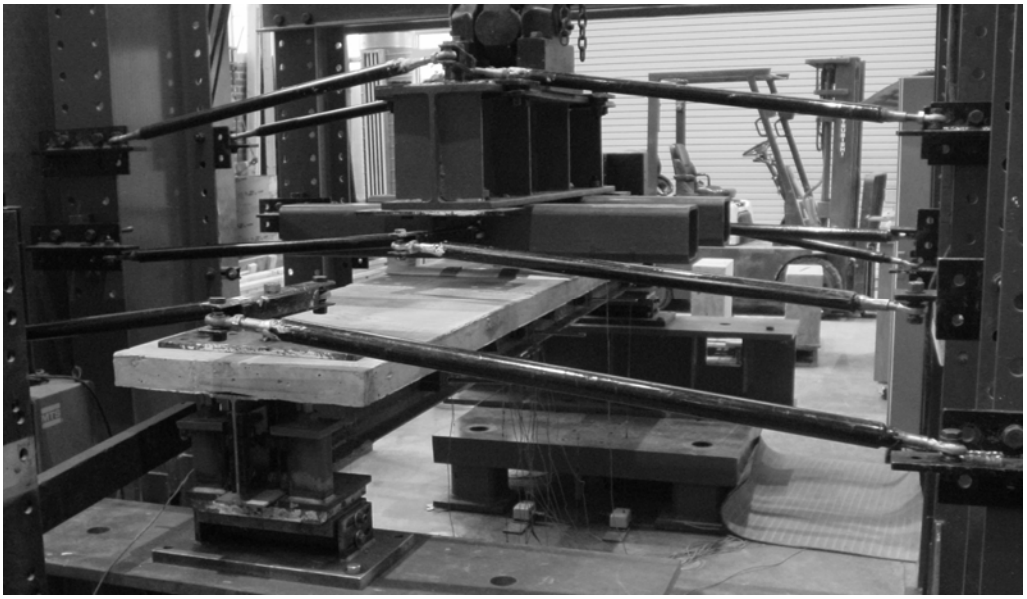

Fig 2: Beam test setup (b) actual

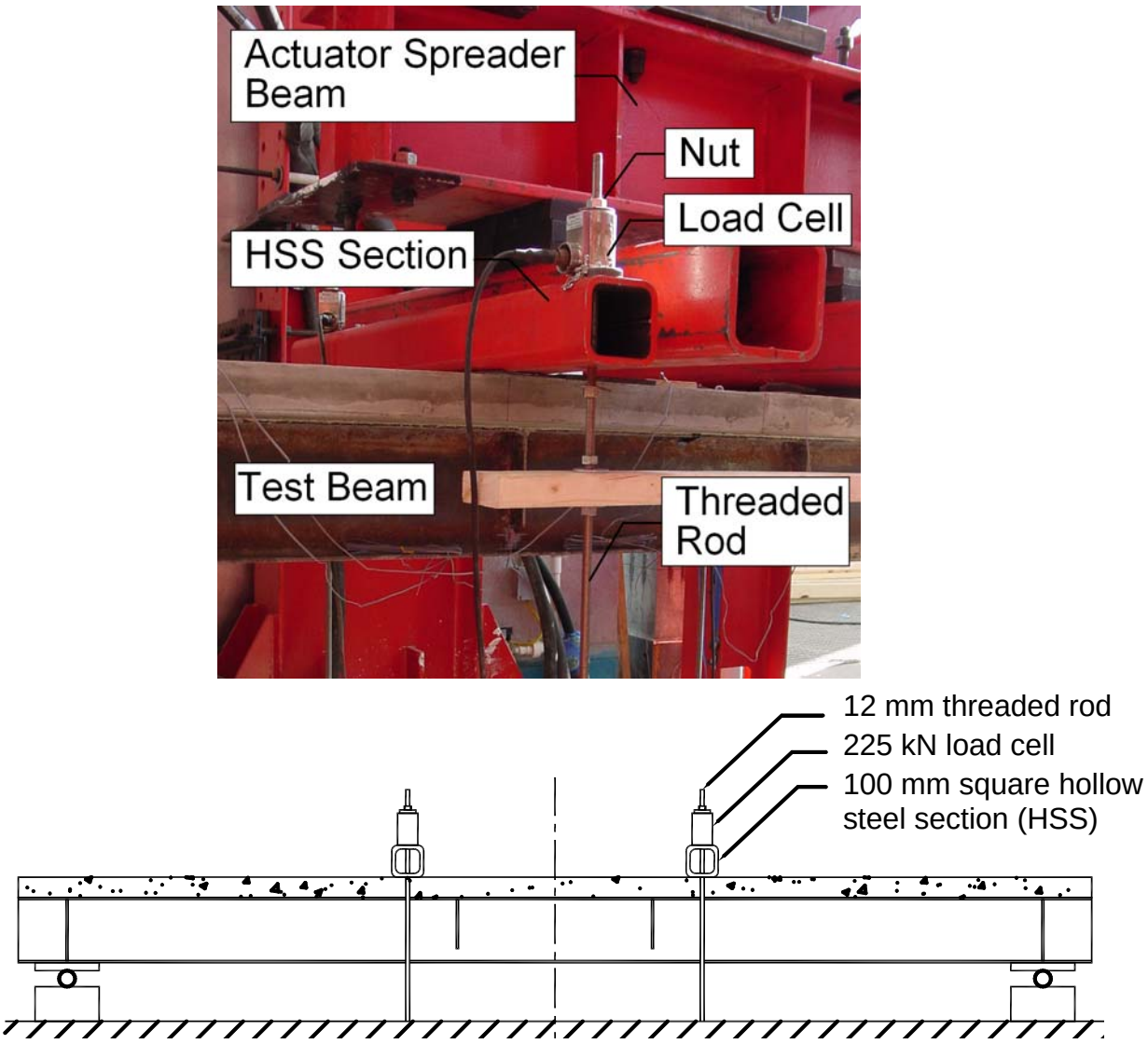

Fig 3: Independent dead-load apparatus

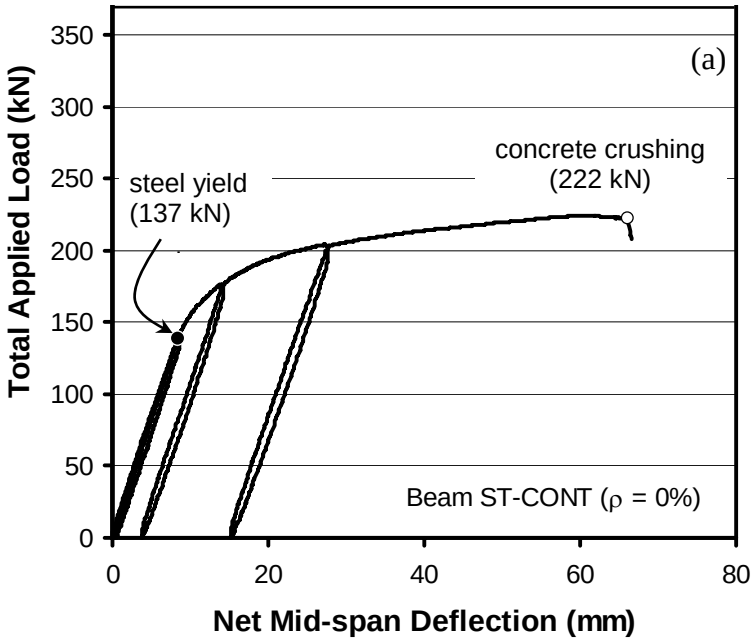

Fig 4: Load-deflection behavior of the three overloading test beams (a) ST CONT (b) OVL-1 (c) OVL-2 (d) typical rupture failure

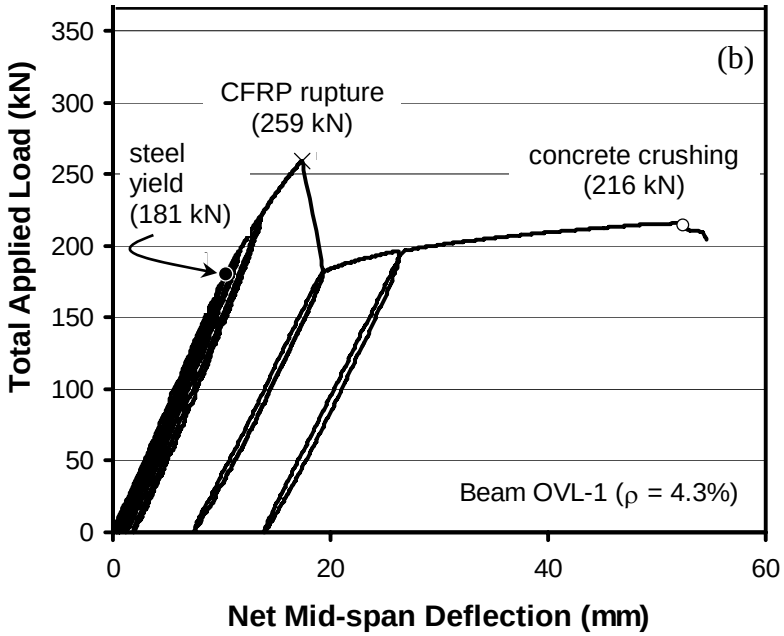

Fig 4: Load-deflection behavior of the three overloading test beams (b) OVL-1

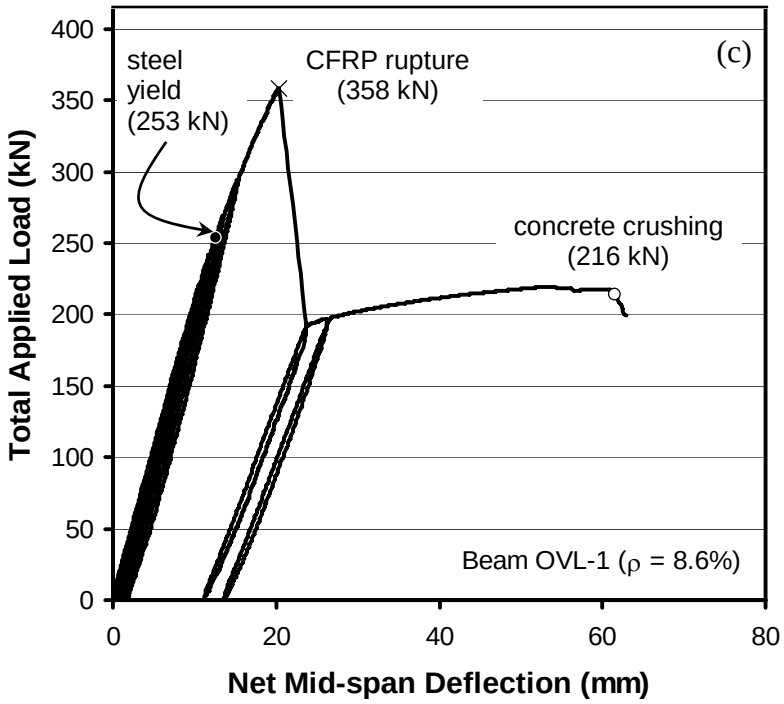

Fig 4: Load-deflection behavior of the three overloading test beams (c) OVL-2

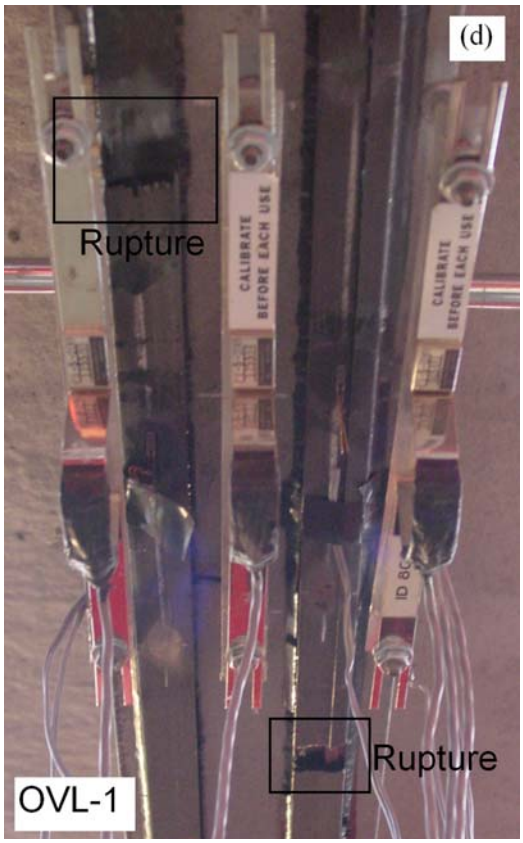

Fig 4: Load-deflection behavior of the three overloading test beams (d) typical rupture failure

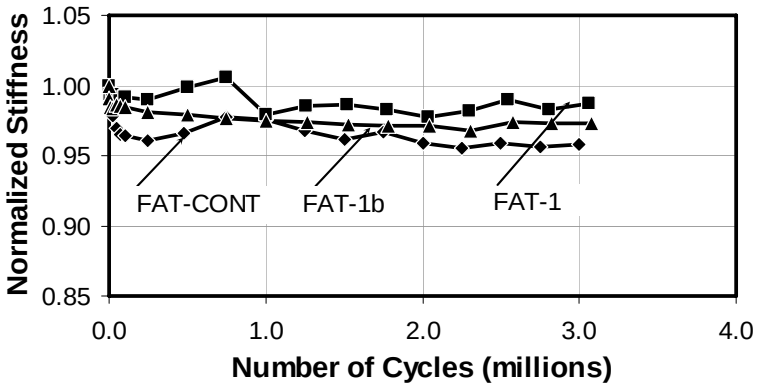

(a) stiffness

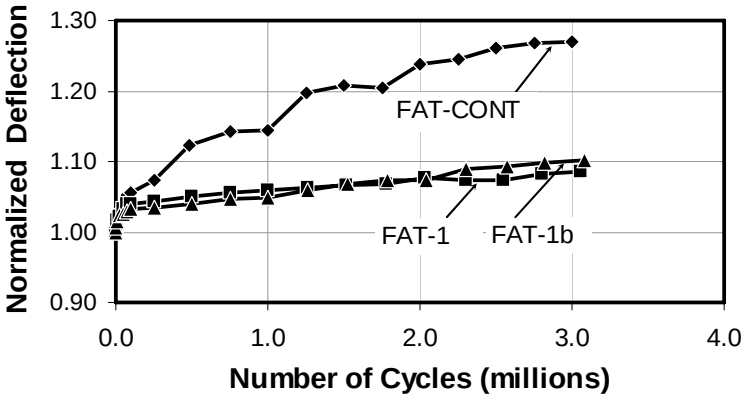

(b) mean deflection

Fig 5: Degradation of (a) stiffness and (b) mean deflection for the fatigue beams

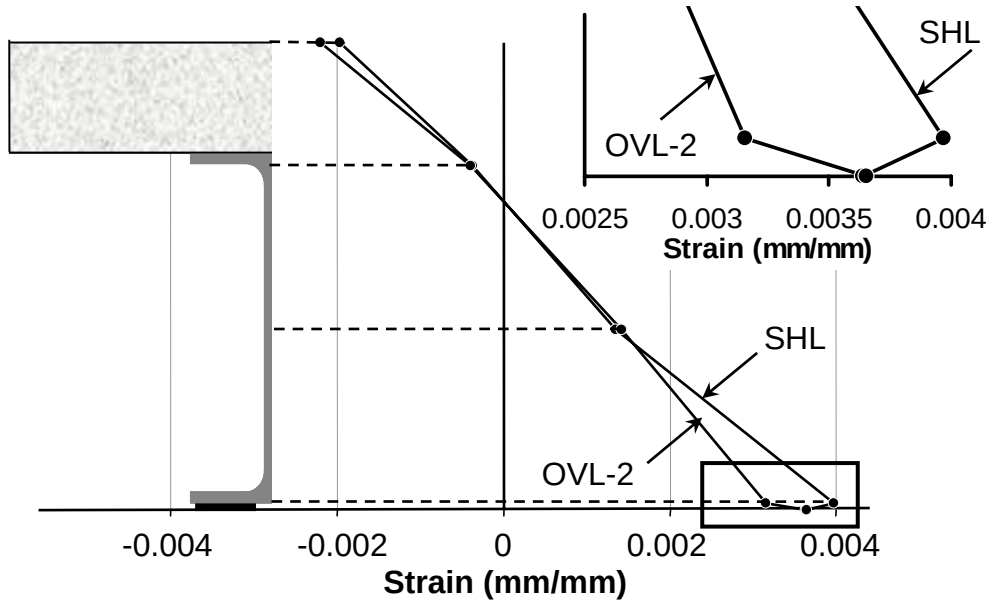

Fig 6: Strain profiles for beam SHL and OVL-2 (ρ = 8.6%)

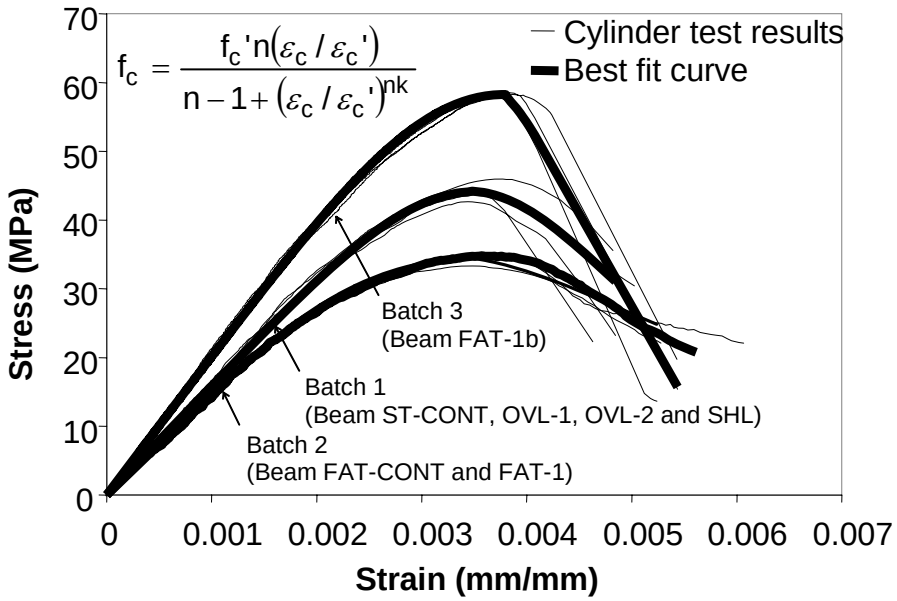

Fig 7: Concrete material properties

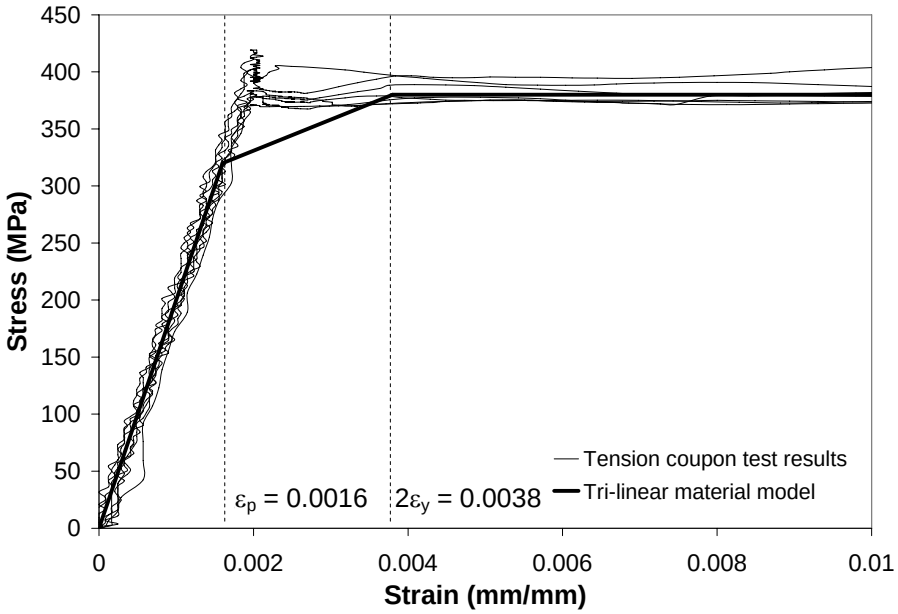

Fig 8: Steel material properties

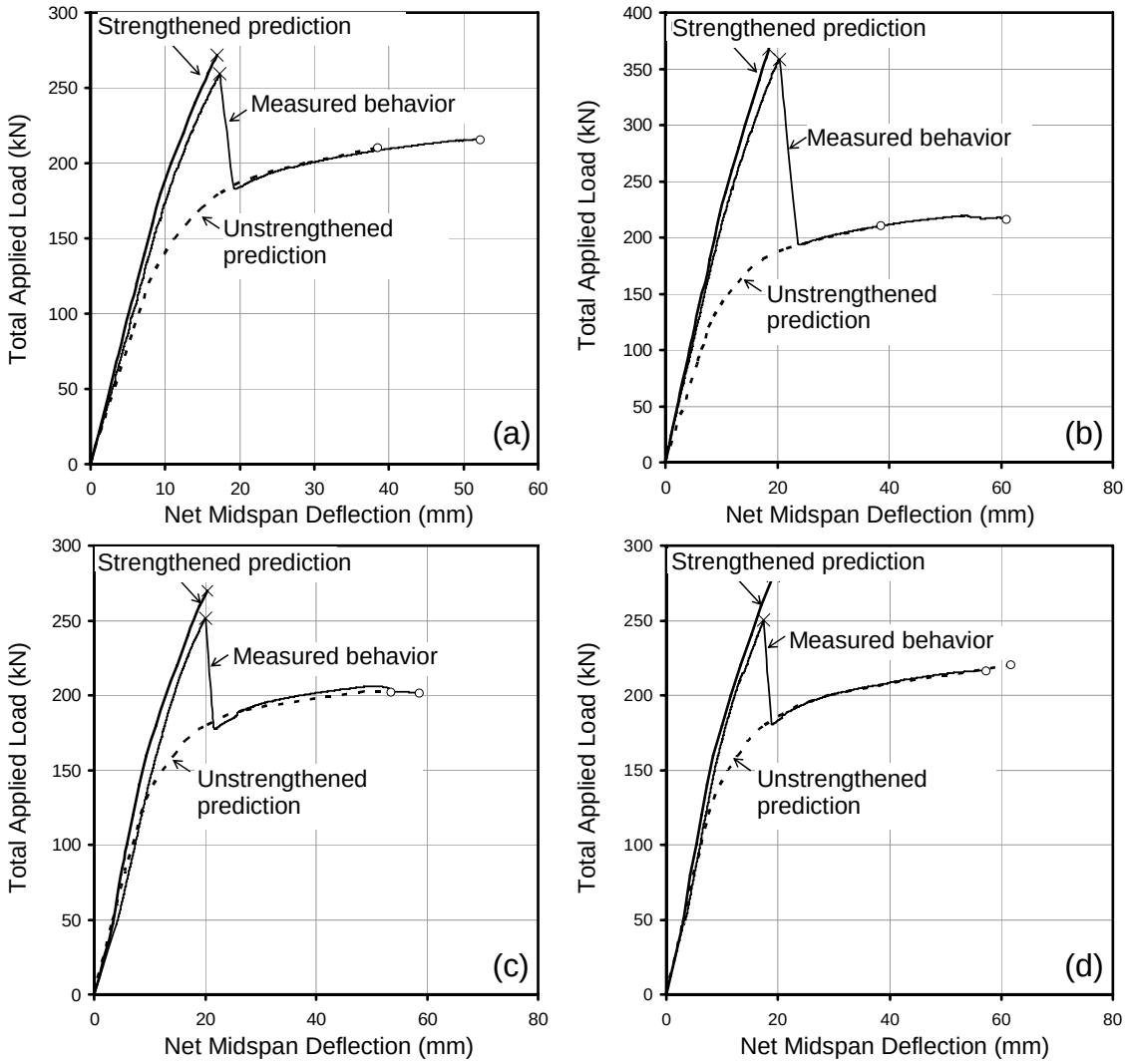

Fig 9: Model verification (a) OVL-2 (ρ = 8.6%) (b) OVL-1 (ρ = 4.3%) (c) FAT-1 (ρ = 4.3%) (d) FAT-1b (ρ = 4.3%)

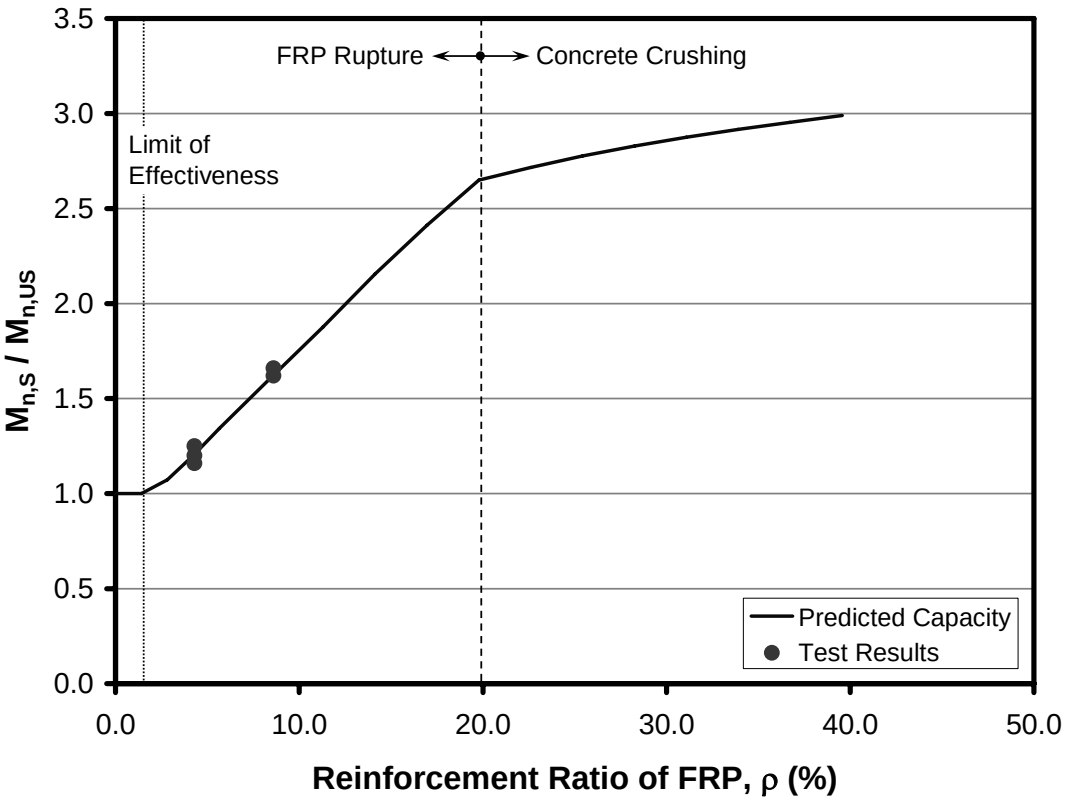

Fig 10: Effect of reinforcement ratio on nominal moment capacity

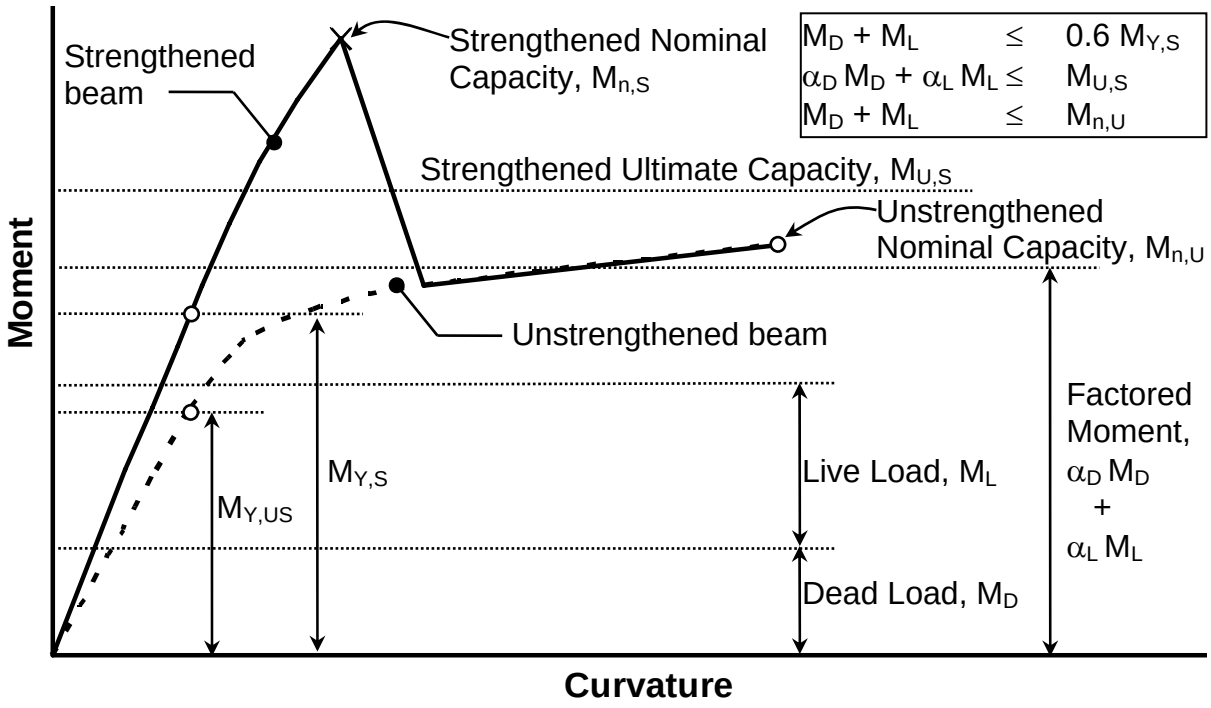

Fig 11: Load levels and moment-curvature behavior for a strengthened beam